

## Experimental observation of percolation-enhanced nonlinear light scattering from semicontinuous metal films

M. Breit,<sup>1</sup> V. A. Podolskiy,<sup>3</sup> S. Grésillon,<sup>1,2</sup> G. von Plessen,<sup>1</sup> J. Feldmann,<sup>1</sup> J. C. Rivoal,<sup>2</sup> P. Gadenne,<sup>5</sup> Andrey K. Sarychev,<sup>3</sup> and Vladimir M. Shalaev<sup>1,3,4</sup>

<sup>1</sup>Photonics and Optoelectronics Group, Physics Department and CeNS, University of Munich, D-80799 München, Germany

<sup>2</sup>Lab. Optique Physique, ESPCI, CNRS-UPR5 and Université P. et M. Curie, 75231 Paris, France

<sup>3</sup>Department of Physics, New Mexico State University, Las Cruces, New Mexico 88003

<sup>4</sup>School of Electrical and Computer Engineering, Purdue University, West Lafayette, Indiana 47907-1285

<sup>5</sup>L.M.O.V., Université de Versailles Saint Quentin, CNRS UMR 8634, F-78035 Versailles, France

(Received 15 May 2001; published 6 September 2001)

Strongly enhanced second-harmonic generation (SHG), which is characterized by a nearly isotropic intensity distribution, is observed for gold-glass films near the percolation threshold. The diffuselike SHG scattering, which can be thought of as nonlinear critical opalescence, is in sharp contrast with highly collimated *linear* reflection and transmission from these nanostructured semicontinuous metal films. Our observations, which can be explained by giant fluctuations of local nonlinear sources for SHG due to plasmon localization, verify recent predictions of percolation-enhanced nonlinear scattering.

DOI: 10.1103/PhysRevB.64.125106

PACS number(s): 72.15.Gd, 05.70.Jk, 42.65.Ky, 78.20.Ci

When metal is evaporated or sputtered onto an insulating substrate and the metal filling factor  $p$  is gradually increased, the coalescence between initially isolated metal granules results in the formation of irregularly shaped fractal clusters of the metal particles. At percolation ( $p = p_c$ ), an extended metal cluster spans over the entire sample, and the insulator-metal phase transition occurs in the film.<sup>1</sup> Metal-dielectric films close to the percolation threshold (also referred to as percolation or semicontinuous films) show remarkable optical properties resulting from disorder-induced localization of plasmons. The plasmon localization leads to the electromagnetic energy being concentrated in sharp nm-sized peaks, “hot spots.” The local fields in such hot spots have been shown to be enhanced enormously, with the intensity  $I_{loc}$  exceeding the applied intensity  $I_0$  by four to five orders of magnitude.<sup>2</sup> The local fields exhibit giant fluctuations over the film in amplitude, phase, and polarization. The local-field enhancements associated with the hot spots are important for amplifying nonlinear optical processes such as surface-enhanced Raman scattering (SERS).<sup>3</sup>

One of most interesting theoretical predictions for percolation films is that nonlinear light scattering at the  $n$ th frequency harmonic  $n\omega$  of an incident beam can be significantly enhanced and it is characterized by a broad, nearly isotropic angular distribution.<sup>4</sup> The enhanced  $n\omega$  diffuse scattering from percolation films was denoted in Ref. 4 as percolation-enhanced nonlinear scattering (PENS). At first glance, the PENS effect is surprising since a nanostructured percolation film is, on average, homogeneous on the micrometer scale, so that there are no wavelength-sized speckles on the film which could result in conventional diffuse light scattering. Indeed, if the inhomogeneity scale  $a$  of local field fluctuations is much smaller than the wavelength  $\lambda$ , the diffuse component in linear scattering, which is  $\sim (a/\lambda)^4 \langle I_{loc} \rangle / I_0$  (the angular brackets stand for averaging over the film), is negligible, since  $(a/\lambda)^4 \ll 1$  and the mean local field, typically, is relatively small,  $\langle I_{loc} \rangle / I_0 \lesssim 1$ . In con-

trast, PENS is caused by the *giant* nm-scale field fluctuations resulting from plasmon localization.<sup>4</sup> The intensity of nonlinear scattering at frequency  $n\omega$  is  $\sim (a/\lambda)^4 \langle (I_{loc}/I_0)^n \rangle$ ; thus the strongly fluctuating local sources for the  $n\omega$  light are enhanced by the factor  $(I_{loc}/I_0)^n$ , which is very large and increases with  $n$ . Hence the role of field fluctuations is dramatically increased for nonlinear scattering. When  $(a/\lambda)^4 \langle (I_{loc}/I_0)^n \rangle \gg 1$ , the total diffuse component in the scattered light from a percolation film can be much larger than the coherent signal radiated in the specularly reflected and transmitted directions.<sup>4</sup> The PENS effect can be thought of as *nonlinear* critical opalescence resulting from Anderson localization of plasmons in the film. The dominance of the diffuse component is in sharp contrast to *linear* light scattering ( $n = 1$ ), which is still expected to be dominated by the highly directional reflected and transmitted beams.<sup>5</sup> Thus the central theoretical prediction for the PENS effect is that percolation metal films should be strongly scattering for nonlinear signals, with a broad, nearly isotropic angular intensity distribution, while for linear scattering the diffuse component, although enhanced, still remains relatively small.

In this article, we experimentally verify the existence of the PENS effect. We show that strongly enhanced second-harmonic generation (SHG), which is characterized by a broad angular distribution, is observed on gold-glass films near the percolation threshold. The diffuselike SHG scattering contrasts with highly directional *linear* reflection and transmission from these nanostructured films. Our observations are in agreement with theoretical calculations of the PENS effect performed here for SHG on gold-glass percolation films.

Samples of percolation metal films were prepared by evaporating gold thin films (10 nm thickness) on a glass substrate at room temperature under ultrahigh vacuum ( $10^{-9}$  Torr).<sup>6</sup> In order to determine how close to the percolation threshold the films were, the resistivity and the deposited mass thickness were measured during film deposition.

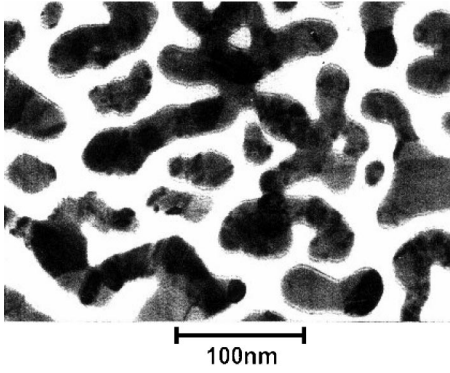


FIG. 1. Transmission electron microscopy (TEM) image of a part of a gold-glass film at the percolation threshold ( $p \approx p_c$ ).

Optical reflection and transmission of the samples were determined outside the vacuum chamber and compared with the known optical properties of percolation samples.<sup>6</sup> Transmission electron microscopy was performed by depositing the same film on a Cu grid covered by a very thin SiO<sub>2</sub> layer. A transmission electron microscope (TEM) image of a part of a percolation gold film is shown in Fig. 1. For comparison, we also deposited smooth continuous gold films under the same deposition conditions.

To obtain SHG from a metal film, we used a pulsed light beam at three different wavelengths  $\lambda_{exc} = 770, 800,$  and  $920$  nm (corresponding to fundamental frequencies  $\omega$ ) generated by a Ti:sapphire laser (pulse duration 150 fs); the beam was focused on a  $4 \times 10^3 \mu\text{m}^2$  area of the film and was incident at  $-45^\circ$  with respect to the film normal, as shown in Fig. 2(a). Measurements were performed for both *s* and *p* polarizations of the incident light. Linear and nonlinear light scattering from the percolation metal film results in coherent beams in the specularly reflected and transmitted directions and also in diffuse light as shown in Fig. 2(a). The scattered light was detected by a photomultiplier using photon counting and interference filters for spectral selection. For comparison, we also studied linear scattering and reflection of incident light at 400 nm and 800 nm. For angular dependence measurements, the photomultiplier was moved around the sample. Light scattering by both percolation and continuous gold films was studied and compared.

Results of our experimental SHG studies obtained on percolation films are shown in Fig. 2(b). Here, coherent SHG signals were detected at  $\lambda_{det} = 400$  nm (corresponding to  $2\omega$ ) in the specularly reflected and transmitted directions,  $45^\circ$  and  $135^\circ$ , respectively. Using a small pinhole in front of the photomultiplier and high angular resolution, these SHG signals were found to have a Gaussian intensity distribution as a function of detection angle, with a narrow width of about  $1^\circ$  (not shown). For *p* polarization of the incident beam, the coherent SHG component radiated in the specularly reflected direction is about 3 times larger than for *s* polarization. This difference indicates that for the specularly reflected signal, the usual dominance of the SHG from *p*-polarized excitation over that from *s*-polarized excitation, which is known from flat continuous metal surfaces,<sup>7</sup> is preserved, to some extent.

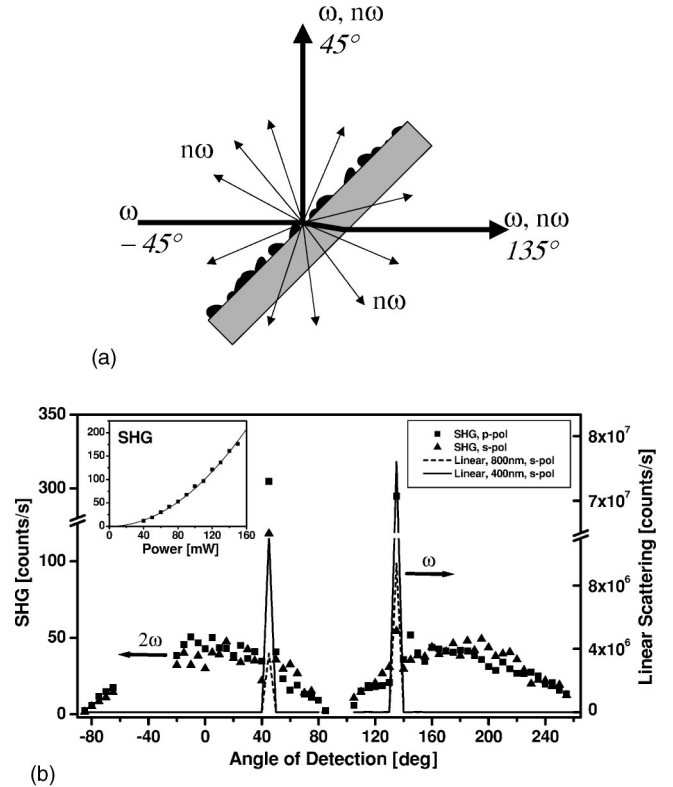


FIG. 2. (a) Linear reflection and transmission at frequency  $\omega$  and diffuselike PENS (at frequency  $n\omega$ ) from a percolation metal-dielectric film. (b) Angular distributions of reflected and transmitted light (lines) and of SHG (symbols) from percolation gold-glass film; the polarizations of the incident light are indicated. The gap in the SHG data near  $-45^\circ$  is due to the geometry of the excitation setup. Inset: intensity dependence for diffuse SHG detected at  $0^\circ$ .

In addition to the coherent SHG component at  $45^\circ$  and  $135^\circ$ , a strong diffuselike signal, characterized by a broad angular distribution, was measured at  $2\omega$ , as seen in Fig. 2(b). The intensity of this diffuse component exhibits the  $I^2$  dependence expected for SHG, as illustrated in the inset of Fig. 2(b) for the normal direction  $0^\circ$ . The total (angle-integrated) intensity of this diffuse SHG component exceeds the intensity of the coherent beam reflected in the specular direction by a factor of 350, for *p*-polarized incident light, and by  $10^3$ , for *s*-polarized light. It is important to note that the highly *diffuse* character of this SHG component is a signature of the predicted PENS effect. Two more observations are also important: The diffuse SHG intensity has roughly a cosine angle dependence, and it is about the same for both *s* and *p* polarizations of the incident beam. Both observations indicate nearly random orientation of the nm-scale nonlinear sources for the diffuse SHG. This conclusion is consistent with Anderson localization of plasmons in percolation films.<sup>2</sup> All SHG measurements described above were also done at the fundamental wavelengths  $\lambda_{exc} = 770$  and  $920$  nm. We obtained qualitatively very similar results (not shown here) as in the case of  $\lambda_{exc} = 800$  nm but with different quantitative ratios of the diffuselike scattered and collimated signal intensities from the percolation film.

For comparison, *linear* scattering of incident light at

$\lambda_{det} = \lambda_{exc} = 400$  nm and 800 nm was also measured on the same gold-glass percolation film [solid and dashed lines in Fig. 2(b), respectively]. In contrast to the SHG signal, the angle-integrated diffuse component is smaller than the components of the linear signal in the reflected and transmitted directions by a factor of 240. In other words, the percolation gold film acts as a nearly perfect (semitransparent) mirror for *linear* scattering. This observation confirms the theoretical expectation that linear scattering from percolation films is much less diffuse than PENS.

Similar measurements of linear and nonlinear light scattering were also performed on *continuous* (i.e., smooth) gold films. As expected for such films,<sup>7,8</sup> both linearly scattered light and SHG were highly collimated in the specularly reflected and transmitted directions (not shown here). The directional characteristics of SHG from continuous gold films thus contrast strongly with those from percolation films, where they are predominantly diffuselike. In addition, the *total*, i.e., angle-integrated, SHG intensity is very different: when compared to the SHG beam reflected from a continuous gold film, the total diffuse SHG intensity from a percolation gold film is greater by a factor of 60, for *p*-polarized incident beam, and by roughly  $10^3$ , for *s* polarization. This enhancement of the total SHG is explained as a consequence of the huge local-field enhancement provided by the plasmon localization in percolation films. Similar comparisons of SHG intensities from percolation and continuous gold films were also performed at other wavelengths: At  $\lambda_{det} = 385$  and 460 nm, we obtained enhancement factors of roughly 50 and 90, respectively, for *p*-polarized SHG. Therefore we can conclude that the enhancement increases toward larger wavelengths. This wavelength dependence will be discussed in more detail in the theoretical part of this paper.

It is worth noting that all experiments reported above were performed below an excitation intensity of  $10^8$  W/cm<sup>2</sup>, where only the fundamental beam at  $\lambda = 800$  nm and SHG at  $\lambda = 400$  nm could be detected; all other spectral components were below the detection limit. However, above  $10^8$  W/cm<sup>2</sup> a continuum background radiation in a broad spectral range was detected. This plasmon-enhanced white light generation was observed earlier in Ref. 9.

To shed more light on our observations, below we extend the theory of the PENS effect from Ref. 4 and apply it to the experiments described above. Specifically, we calculate the diffuse component of SHG from a percolation gold film and compare it with the specularly reflected SHG from both percolation and continuous gold films. The theory supports our explanation of the experimental observations in terms of PENS.

By using the standard approach of scattering theory,<sup>5</sup> we obtain that the integral scattering intensity in all but specular directions is given by  $S = (4k^2/3c) \int (\langle \mathbf{j}_{\mathbf{r}_1}^{(n)} \cdot \mathbf{j}_{\mathbf{r}_2}^{(n)*} \rangle - |\langle \mathbf{j}^{(n)} \rangle|^2) d\mathbf{r}_1 d\mathbf{r}_2$ , where  $k = \omega/c$ , and  $\mathbf{j}^{(n)}$  is a nonlinear local current serving as a local source for the scattered light. As in Ref. 5, we assume that the integrand vanishes for distances  $r \ll \lambda$ , where  $\mathbf{r} = \mathbf{r}_2 - \mathbf{r}_1$ ; therefore, we omit the  $\exp(i\mathbf{k} \cdot \mathbf{r})$  term.

The nonlinear local currents  $\mathbf{j}^{(n)}$  are strongly enhanced in areas of plasmon localization. As discussed above, these extremely sharp peaks of nonlinear light sources are spatially separated on the film. Because of the gigantic spatial fluctuations, the diffuse component of the  $n\omega$  scattering can be estimated as  $\langle \mathbf{j}_{\mathbf{r}_1}^{(n)} \cdot \mathbf{j}_{\mathbf{r}_2}^{(n)*} \rangle \sim \langle |\mathbf{j}^{(n)}|^2 \rangle \propto \langle |\epsilon_{n\omega} E_{n\omega}|^2 |E_\omega|^{2n} \rangle$ . This component is much larger than the coherent (collimated) component  $|\langle \mathbf{j}^{(n)} \rangle|^2 \propto \langle |\epsilon_{n\omega} E_{n\omega} E_\omega^n|^2 \rangle$ . In these formulas and below, the local dielectric constant  $\epsilon_{n\omega}$  takes values of  $\epsilon_{m,n\omega}$  (with probability  $p$ ) and  $\epsilon_d$  (with probability  $1-p$ ) for the metal and dielectric, respectively. Note also that we take into account enhancement for the fields at both fundamental frequency  $\omega$  and generated frequency  $n\omega$ .

PENS can formally be written as<sup>4</sup>  $S = G^{(n)} I_{n\omega}$ , where  $I_{n\omega}$ , in the case under consideration, is the signal intensity from a continuous metal film and  $G^{(n)}$  is the enhancement factor for a semicontinuous film. Thus,  $G^{(n)}$  gives the ratio of the nonlinear signals from “broken” and “perfect” mirrors, representing semicontinuous and continuous films, respectively. As follows from the consideration above, the diffuse part of enhancement,  $G_{dif}^{(n)}$ , strongly exceeds the collimated part,  $G_c^{(n)}$ , so that  $G^{(n)} \approx G_{dif}^{(n)}$  and it is estimated as:<sup>4</sup>

$$G_{dif}^{(n)} \approx (ka)^4 \frac{\langle |\epsilon_{n\omega} E_{n\omega}|^2 |E_\omega|^{2n} \rangle}{|\epsilon_{m,n\omega} E_{n\omega}^{(0)}|^2 |E_\omega^{(0)}|^{2n}}, \quad (1)$$

where  $E_\omega^{(0)}$  and  $E_{n\omega}^{(0)}$  are the applied (probed) fields at the fundamental and generated frequencies.

Although the “Rayleigh factor”  $(ka)^4$  in Eq. (1) is typically small [for our films with  $a \approx 50$  nm, where  $a$  is a typical “in-plane” size of metal grains,  $(ka)^4 \approx 2 \times 10^{-2}$ ], the resultant field-enhancement factor for nonlinear scattering, with  $n \geq 2$ , can still be very large. This is in contrast to linear scattering ( $n = 1$ ) where the specularly reflected component for semicontinuous metal films, typically, exceeds the diffuse scattering.<sup>5</sup> With increase of the order of nonlinearity, enhancement factors increase for both diffuse and collimated scattering, but the diffuse component increases at much greater rates. As a result, PENS is essentially a nonlinear effect and becomes progressively larger for higher nonlinearities.

For comparison, we also give the enhancement factor  $G_c^{(n)}$  for the collimated  $n\omega$  signal on a semicontinuous film (as compared to a continuous film):

$$G_c^{(n)} = \frac{|\langle \epsilon_{n\omega} E_{n\omega} E_\omega^n \rangle|^2}{|\epsilon_{m,n\omega} E_{n\omega}^{(0)}|^2 |E_\omega^{(0)}|^{2n}}. \quad (2)$$

The PENS effect can formally be expressed as  $G_{dif}^{(n)} \gg G_c^{(n)}$ .

In estimates below we use the Drude formula for a dielectric constant of metal  $\epsilon_m(\omega) = \epsilon_0 - (\omega_p/\omega)^2 / [1 + i\omega_\tau/\omega]$ , where  $\epsilon_0$  is a contribution to  $\epsilon_m$  due to interband transitions. For gold,  $\epsilon_0 = 7$ ,  $\omega_p = 9.2$  eV, and  $\omega_\tau = 0.06$  eV; for glass,  $\epsilon_d = 2.2$ . First we estimate  $G_c^{(n)}$ . Since there is little correlation in the field distribution at  $\omega$  and  $n\omega$  we can use the decoupling  $\langle \epsilon_{n\omega} E_{n\omega} E_\omega^n \rangle \rightarrow \langle \epsilon_{n\omega} E_{n\omega} \rangle \langle E_\omega^n \rangle$ . Then we estimate  $\langle \epsilon_{n\omega} E_{n\omega} \rangle \equiv \epsilon_{e,n\omega} E_{n\omega}^{(0)} = \sqrt{\epsilon_{m,n\omega} \epsilon_d} E_{n\omega}^{(0)}$ , where we used the exact result for the effective dielectric constant  $\epsilon_e$  in a  $2d$  percolation system:  $\epsilon_e = \sqrt{\epsilon_m \epsilon_d}$ . Using then the

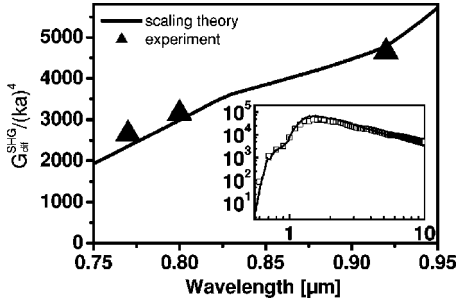


FIG. 3. Normalized PENS enhancement factor for SHG,  $G_{dif}^{SHG}/(ka)^4$ , as a function of wavelength for a percolation gold-glass film. The solid line is the result of theoretical formula (4). The solid triangles are the enhancement factor determined from SHG measurements at the fundamental wavelengths 770, 800, and 920 nm. Inset: theoretical data of the normalized PENS enhancement factor for SHG over a broad spectral range. The solid line is the result of theoretical formula (4), and the squares are the results of numerical simulations based on Eq. (1).

estimate for  $\langle E_\omega^n \rangle$  (see Ref. 2), we find that  $G_c^{(n)} \sim \epsilon_m^{n^2} |\epsilon_m, \omega|^{n-3} / (\epsilon_m^{n, n\omega} \epsilon_d^{n-2})$ . With the Drude formula for  $\epsilon_m$ , we find that  $G_c^{(n)} \sim (n^2/\epsilon_d^{n-2}) \omega_p^{2(n-2)} \omega_\tau^2 / \omega^{2(n-1)}$ ; i.e., for  $n > 2$ , it reaches the maximum  $G_c^{(n)} \sim (n^2/\epsilon_d^{n-2}) (\omega_p/\omega_\tau)^{2(n-2)} \gg 1$  at  $\omega \sim \omega_\tau$ . The estimates show that the collimated nonlinear signal from a semicontinuous metal film is enhanced in comparison with a continuous metal film, for third and higher harmonics, but not for SHG. Indeed, experimentally we find  $G_c^{SHG} \approx 0.1$ .

By applying the scaling analysis of Ref. 2 to Eq. (1), we obtain the following estimate for the diffuse PENS:

$$\frac{G_{dif}^{(n)}}{(ka)^4} \approx (a/\xi_A)^{4n} \frac{|\epsilon_m, n\omega|^{1/2} |\epsilon_m, \omega|^{3(n-1/2)}}{\epsilon_d^{n-1} \epsilon_m^{n, n\omega} \epsilon_m^{n-1}}, \quad (3)$$

where  $a$  is the grain size and  $\xi_A$  is the Anderson localization length in the special case of  $\epsilon_m = -\epsilon_d$ . According to Eq. (3) PENS rapidly disappears if there is no plasmon localization, i.e., if  $\xi_A/a \rightarrow \infty$ . For estimates below we use  $\xi_A/a \approx 1.6$ , which is consistent with our previous simulations and experimental measurements.<sup>2</sup>

For SHG ( $n=2$ ) formula (3) gives the estimate

$$\frac{G_{dif}^{SHG}}{(ka)^4} \approx (a/\xi_A)^8 \frac{|\epsilon_m, 2\omega|^{1/2} |\epsilon_m, \omega|^{9/2}}{\epsilon_d \epsilon_m^{n, 2\omega} \epsilon_m^{n-3}}, \quad (4)$$

which with the use of the Drude formula gives  $G_{dif}^{SHG}/(ka)^4 \approx (4/\epsilon_d)(a/\xi_A)^{10} [\omega_p^2 \omega^2 / (\omega_\tau^4)]$ .

The normalized PENS factor for SHG,  $G_{dif}^{SHG}/(ka)^4$ , obtained from the scaling analysis according to Eq. (4) is shown in Fig. 3 as a function of the wavelength. The PENS factor increases with wavelength. The physical explanation for this behavior is that the local fields generating the SHG enhancement increase towards longer wavelengths.<sup>2</sup> In addition to the results from the scaling analysis, the enhancement factors obtained from the SHG measurements at fundamental wavelengths  $\lambda_{exc} = 770, 800, 920$  nm with  $p$  polarization are plotted. The predictions of the scaling theory are in good

agreement with our experimental results. The increase of the enhancement factor with wavelength experimentally observed here thus confirms the wavelength dependence of the local fields predicted by the theory in Ref. 2.

The inset in Fig. 3 shows the theoretical results over a wider wavelength range. In addition to the results of the scaling analysis, also the results from numerical simulations which were performed using the real-space renormalization group described in detail in our previous publications (see, for example, Ref. 2) are shown. As seen in the inset of Fig. 3, the results of the two calculations are in good accord. Both calculations predict a flattening of the wavelength dependence of  $G_{dif}^{SHG}/(ka)^4$  beyond  $\sim 1.5 \mu\text{m}$ , and a subsequent slight decrease. This behavior is due to the fact that for very large wavelengths, the rate at which the diffuse SHG from a semicontinuous metal film increases with  $\lambda$  is less than the rate of increase for collimated SHG from a continuous metal film, so that the ratio of these two SHG intensities becomes smaller.

We also compare the diffuse scattering for linear Rayleigh scattering,  $G_{dif}^{(1)}$ , with the PENS at  $2\omega$ ,  $G_{dif}^{(2)} = G_{dif}^{SHG}$ . For  $\lambda_{exc} = 800$  nm, for example, we detected in our experiments that  $G_{dif}^{(1)} = 0.012$  and  $G_{dif}^{SHG} = 63$ , so that for their ratio we have  $G_{dif}^{SHG}/G_{dif}^{(1)} = 5250$ . This enhancement results mainly from the enhancement of the local field at the fundamental frequency at  $\lambda = 800$  nm; therefore, for simplicity, we neglect the small enhancement at  $\lambda/2 = 400$  nm. Then, the theory predicts that  $G_{dif}^{SHG}/G_{dif}^{(1)} = \langle |E/E_0|^4 \rangle / \langle |E/E_0|^2 \rangle \sim |\epsilon_m|^3 / (\epsilon_d \epsilon_m^{n^2}) \sim 10^4$ , for 800 nm (where  $E_0$  is the applied field). Thus, our experimental observations, in accord with theory, imply that the fourth order of the field enhancement exceeds the second order by roughly four orders of magnitude. To our best knowledge, this is the first direct observation of the increase of optical enhancement with the order of optical nonlinearity.

It is worth noting that PENS is anticipated to be a robust effect. As predicted in Ref. 2, the enhanced nonlinear scattering resulting from localized plasmons can occur provided that the field correlation length is smaller than the percolation length characterizing the mean size of fractal metal clusters on the film. This condition results in the following estimate for a metal concentration range  $\Delta p = p - p_c$ , where the effect occurs:<sup>2</sup>  $\Delta p \leq \epsilon_d^{3/8} (\omega/\omega_p)^{3/4}$ . As follows from this estimate,  $\Delta p$  shrinks when the frequency decreases. However, in the visible and near-infrared ranges, PENS is calculated to occur within a broad range of  $p$ , even relatively far from  $p_c$ . The reason for this robustness is the fact that in the optical range the displacement current dominates the Ohmic current so that the physical contact between particles is of no critical importance. Thus, it may be possible that the ‘‘unusually’’ large diffuse SHG component reported in earlier studies of SHG from metal-dielectric films relatively far from percolation<sup>10–12</sup> is related to the PENS effect reported here. We have checked the robustness of the PENS effect by performing additional angle-resolved SHG experiments on semicontinuous metal films with  $p \approx p_c$  and  $p > p_c$ . Figure 4 shows the angular distribution of the SHG signal from three different semicontinuous gold films. Two of them have metal

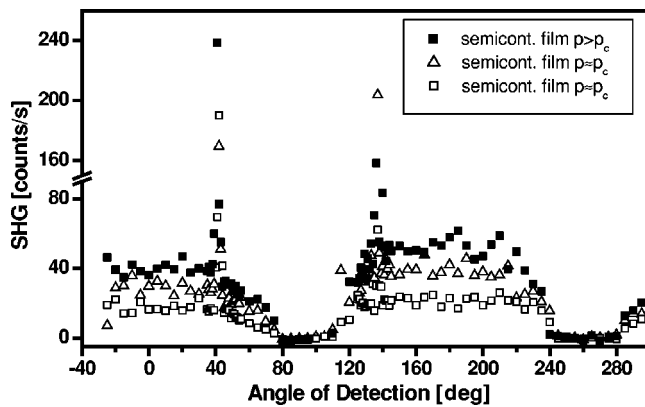


FIG. 4. Angular distribution of the SHG from semicontinuous metal films with different metal concentrations  $p$ : at the percolation threshold  $p \approx p_c$  (open squares and triangles) and slightly above the percolation threshold  $p > p_c$  (solid squares).

concentrations at the percolation threshold (shown as open squares and triangles in Fig. 4) and one film has a metal concentration slightly above the percolation threshold, as checked by resistivity and mass thickness measurements during deposition (solid squares in the plot). The qualitative angle dependence and size of the SHG intensity are similar in all three cases, demonstrating that PENS is a reproducible effect and robust against small variations of the metal concentration  $p$ .

PENS is expected to occur within a broad spectral range because of the unique properties of plasmons in percolation films. The resonant frequencies of localized plasmon modes depend on the local structure of metal clusters in the areas of plasmon localization. The scale-invariant geometry of a percolation composite results in a large variety of shapes and sizes of the resonating structures (from the size of particles to the size of the infinite cluster). The variety of these structures supporting the localized plasmon excitations results, in turn, in an unusually broad spectral range covered by the plasmon modes of percolation films, from the near ultraviolet to the far infrared.<sup>2</sup> This is in sharp contrast with plasmon modes of individual metal particles and compact metal structures that typically lie in the visible.

To summarize, we have observed the predicted PENS effect. We have found strongly enhanced nonlinear scattering in SHG from percolation gold-glass films which show little linear (diffuse) scattering. The observations, including the absolute size and the wavelength dependence of the PENS effect, are in good accord with theoretical predictions. We note that the light with a broad angular distribution resulting from PENS is similar to that produced by random lasers and might be of interest for various applications, e.g., in enhanced light-emitting devices.

This work was supported in part by the DFG (SFB 486, PI261/3-1 and Leibniz Award), NSF (DMR-9810183), ARO (DAAG55-98-1-0425), PRF (ACS-PRF-35028-AC5), and the AvH Foundation.

<sup>1</sup>D.J. Bergman and D. Stroud, in *Solid State Physics*, (Academic, New York, 1992), Vol. 46, p. 147; D. Stauffer and A. Aharony, *Introduction to Percolation Theory*, 2 ed. (Taylor & Francis, Philadelphia, 1991).

<sup>2</sup>V.M. Shalaev and A.K. Sarychev, *Phys. Rev. B* **57**, 13265 (1998); S. Grésillon, L. Aigouy, A.C. Boccard, J.C. Rivoal, X. Quelin, C. Desmarest, P. Gadenne, V.A. Shubin, A.K. Sarychev, and V.M. Shalaev, *Phys. Rev. Lett.* **82**, 4520 (1999); A.K. Sarychev, V.A. Shubin, and V.M. Shalaev, *Phys. Rev. B* **60**, 16389 (1999); V.M. Shalaev, *Nonlinear Optics Of Random Media: Fractal Composites and Metal-Dielectric Films* (Springer, Heidelberg, 2000).

<sup>3</sup>P. Gadenne, F. Brouers, V.M. Shalaev, and A.K. Sarychev, *J. Opt. Soc. Am. B* **15**, 68 (1998).

<sup>4</sup>A.K. Sarychev, V.A. Shubin, and V.M. Shalaev, *Phys. Rev. E* **59**, 7239 (1999); A.K. Sarychev and V.M. Shalaev, *Phys. Rep.* **335**, 275 (2000).

<sup>5</sup>F. Brouers, S. Blacher, and A.K. Sarychev, *Phys. Rev. B* **58**,

15897 (1998).

<sup>6</sup>Y. Yagil, P. Gadenne, C. Julien, and G. Deutscher, *Phys. Rev. B* **46**, 2503 (1992); P. Gadenne, Y. Yagil, and G. Deutscher, *J. Appl. Phys.* **66**, 3019 (1989).

<sup>7</sup>N. Bloembergen, R.K. Chang, S.S. Jha, and C.H. Lee, *Phys. Rev.* **174**, 813 (1968).

<sup>8</sup>Y.R. Shen, *The Principles of Nonlinear Optics* (Wiley, New York, 1984).

<sup>9</sup>S. Ducourtieux, S. Grésillon, A.C. Boccard, J.C. Rivoal, X. Quelin, P. Gadenne, V.P. Drachev, W.D. Bragg, V.P. Safonov, V.A. Podolskiy, Z.C. Ying, R.L. Armstrong, and V.M. Shalaev, *J. Nonlinear Opt. Phys. Mater.* **9**, 105 (2000).

<sup>10</sup>C.K. Chen, A.R.B. de Castro, and Y.R. Shen, *Phys. Rev. Lett.* **46**, 145 (1981).

<sup>11</sup>O.A. Aktsipetrov, O. Keller, K. Pedersen, A.A. Nikulin, N.N. Novikova, and A.A. Fedyanin, *Phys. Lett. A* **179**, 149 (1993).

<sup>12</sup>L. Kuang and H.J. Simon, *Phys. Lett. A* **197**, 257 (1995).